

# LOADING AND UNLOADING TEST OF HARD ROCK AND ITS ELASTOPLASTIC DAMAGE COUPLING MODEL

# OBREMENILNI IN RAZBREMENILNI PREIZKUS TRDNIH KAMNIN IN NJIHOV ELASTOPLASTIČNI MODEL POŠKODBE KONTAKTA

**Zhen Li** (corresponding author)

Henan Polytechnic University,  
School of Civil Engineering,  
Jiaozuo, Henan 454000, China  
E-mail: zhenli@hpu.edu.cn

**Dongdong Zhang**

Yankuang Group Company Limited,  
Yanzhou Coal Ordos Neng Hua Company Limited,  
Ordos, Inner Mongolia Autonomous Region  
017000, China

**Shuang Zhao**

Yankuang Group Company Limited,  
Yanzhou Coal Ordos Neng Hua Company Limited,  
Ordos, Inner Mongolia Autonomous Region  
017000, China

**DOI** <https://doi.org/10.18690/actageotechslov.15.2.38-46.2018>

## Keywords

high stress; hard rock; loading and unloading test; coupling model

## Ključne besede

visoka napetost; trdna kamnina; obremenilni in razbremenilni preizkus; model kontakta

## Abstract

*Deep-buried engineering and test results show that hard rocks behave as part of an elastoplastic damage coupling process. The coupling effect can contribute to the weakness of the surrounding rocks and the extension of the water channels. As a result, the coupled elastoplastic damage model is the basis for a stability analysis in deep engineering. In this paper loading and unloading tests were conducted on  $T_{2b}$  marble in the Jinping II hydropower station. Based on the tests the effects of the confining pressure on the strength, the failure strain and the dilation were analyzed. According to the plastic shear failure and the parameters weakness mechanism, the damage-evolution function reflecting the weakness character, the loading function and the plastic potential function regarding plastic hardening were proposed. The activation of the damage and plastic process was then studied. The coupled elastoplastic damage model was finally established. Through simulating the test curve, the proposed model was verified. This model could play an important role in the stability analysis of deep-buried hard-rock engineering.*

## Izvleček

*Globoko vkopani inženirski objekti in rezultati preizkusov kažejo, da se trdne kamnine obnašajo kot del elastoplastičnega procesa poškodbe kontakta. Vpliv na intaktnost kontakta lahko prispeva k šibkosti okoliških kamnin in razširitvi vodnih kanalov. Rezultat tega je, da je elastoplastični model poškodbe kontakta osnova za analizo stabilnosti pri globoko vkopanih inženirskih objektih. V prispevku smo na marmorju  $T_{2b}$  na hidroelektrarni Jinping II izvedli obremenilne in razbremenilne preizkuse. Na podlagi preizkusov smo analizirali učinke hidrostatskega tlaka na trdnost, specifično deformacijo pri porušitvi in dilatacijo. Glede na plastično strižno porušitev in mehanizem slabosti parametrov smo predlagali funkcijo razvijanja poškodb, ki odraža značilnost šibkosti, obremenilno funkcijo in funkcijo plastičnega potenciala pri plastičnem utrjevanju. Nato smo proučevali aktivacijo poškodb in plastičnih procesov. Končno je bil ugotovljen povezani model elastoplastične poškodbe. Predlagan model je bil preverjen s simulacijo preizkusne krivulje. Ta model bi lahko imel pomembno vlogo pri analizi stabilnosti globoko vkopanih inženirskih objektov v trdnih kamninah.*

## 1 INTRODUCTION

To deal with the potential problems associated with a shortage of energy supply, many hydropower stations and transportation tunnels are being built in China, implementing the western development strategy project. The huge rock engineering located in high mountains in the west of China, have characters such as deep buried, high stress and long span. For example, the diversion tunnel in the Jinping II hydropower station has a maximum length of 16.6km, an excavation diameter of 13m, a general buried depth of 1500~2000m and a maximum buried depth exceeding 2500m. In this case its high initial geostress and water pressure add difficulties to the construction. Besides these, the diversion tunnel goes through the Jinping mountain and various rock layers. The rock mass has many fractures and water flowing structures. The maximum water pressure exceeds 10MPa[1]. During the excavation of the auxiliary tunnels, the rockburst and water gushing problems resulted in a lot of loss and damage (see Fig.1) [2]. Therefore, the disaster prevention and control in the high geostress and water pressure are the key problems in the construction of deep buried tunnels.



**Figure 1.** Rock-burst and water-gushing problems in deep buried hard rock in the Jinping II hydropower station: (a) strong rock burst (b) high-pressure and large-volume groundwater infiltration.[2].

In the case of high geostress, the behavior of hard rock has its special characters: a) it has the ductility characters in high confining pressure in contrast to the brittleness in the low confining pressure[3]; b) the Mohr-Coulomb criterion applying to the shallow buried rock cannot be used in the deep buried rock with non-linear characters[4]; and c) the elastoplastic deformation becomes more complex. Under the applied force, the microfissures extend and penetrate. On one hand, the strength of the surrounding rock weakens with additional strain generation. On the other hand, the connected fissures act as the water-gutting channels. Therefore, the plastic deformation and damage to the rock have a coupling effect. The coupled elastoplastic damage analysis is the basis for solving the stability problem of deep buried tunnels.

In the triaxial test the microfissures propagate with the increasing load. Material damage accumulates due to the plastic process. Meanwhile, the damage leads to further irreversible plastic deformation, a non-linear constitutive relationship, a strain-softening material and dilation. These mechanical phenomena can be viewed as the coupling effect of damage and plasticity, which is described by continuum damage mechanics and plasticity theory, respectively[5]. Salari et al.[6] formulated a constitutive model in the framework of continuum thermodynamics using internal variables. Chiarelli et al.[7] proposed that the plastic deformation and anisotropy damage are coupled using a triaxial test with claystones. Zhu et al.[8] formulated a micromechanics-based constitutive model for granular materials like sands under a relatively low confining pressure. Zhou and Zhu[9] developed an elasto-plastic damage constitutive model with double yield surfaces for the soft rock.

The existing research was mostly focused on the elastoplastic damage coupling problems in soft rock, while research on the hard rock with deep buried high stresses is still not sufficient. In this paper we made an analysis of the mechanical behavior of the hard rock based on the test results. The coupled elastoplastic damage model was proposed and validated. The work acts as the basis for a study on the weakening process of the surrounding rocks and the formulation of water-gushing fissures.

## 2 TEST ANALYSIS

### 2.1 Test methods and results

The standard cylinder marble samples with sizes of 50×100 mm were made from the marble core buried 2500 m underground in the Jinping II hydropower station diversion tunnel in the Sichuan province of

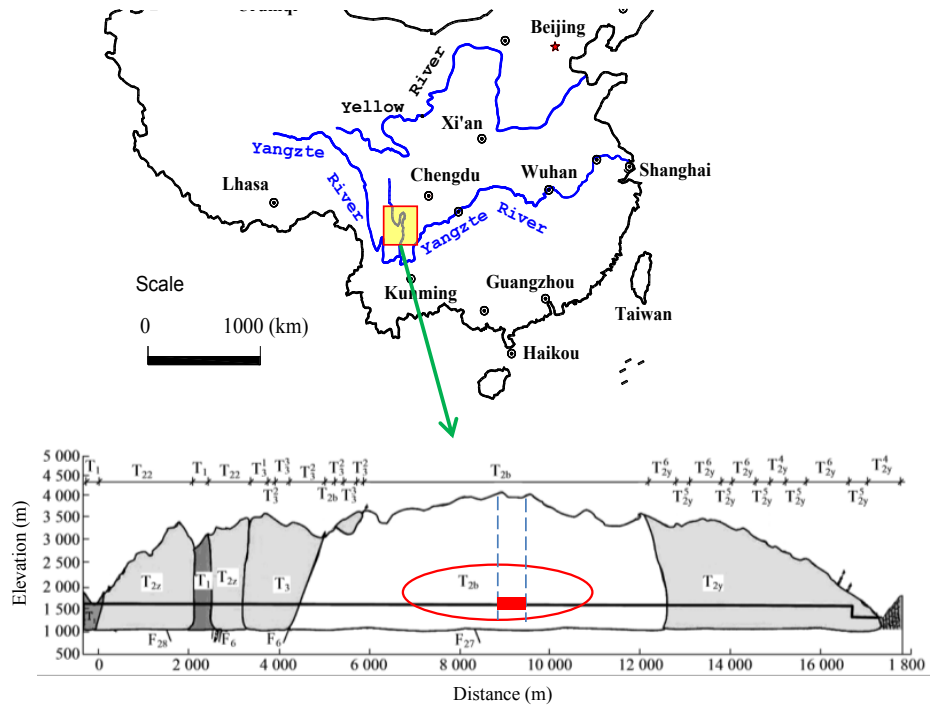


Figure 2. Location of the  $T_{2b}$  marble in the Jinping II hydropower station.

China (see Fig.2). For the purposes of getting the elastic parameters at a different loading stage, a loading-unloading triaxial test was conducted on the MTS815.03 test machine. In order to avoid the sudden energy release and brittle failure caused by post-peak unloading of rock in an unstable state, a special control method was used (see Fig.3). The confining pressure was increased by 1 MPa, followed by an unloading process during which the extra confining pressure was again decreased.

The loading process is controlled by deformation and the loading rate is 0.06 mm/min. The unloading process is controlled by the axial stress and the unloading rate is 26MPa/min. At the end of each unloading the deviatoric pressure is close to 5MPa. Fig.4 shows the stress-strain

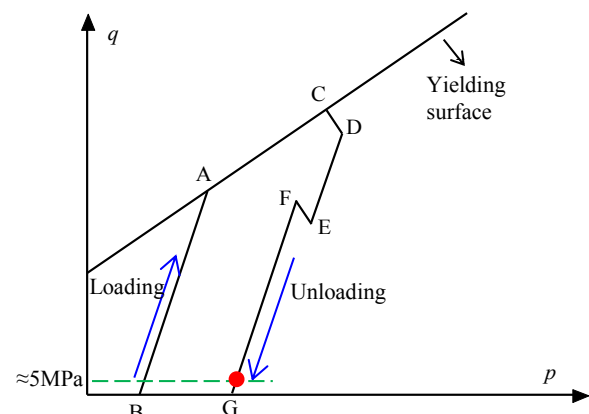


Figure 3. Loading and unloading stress path in the  $p$ - $q$  plane.

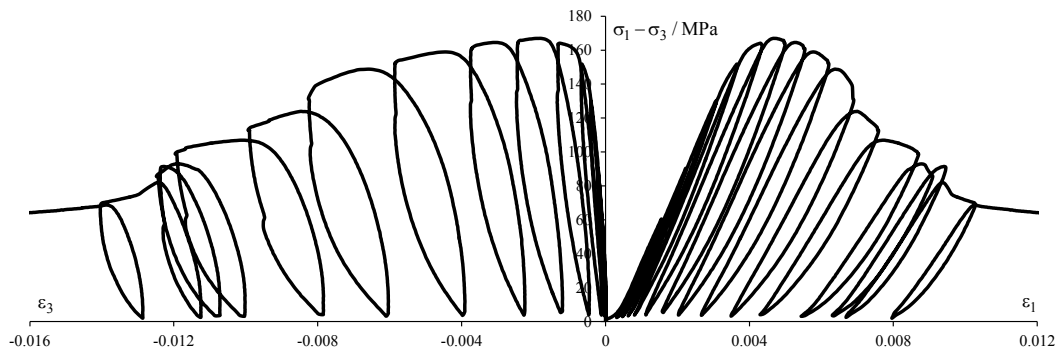
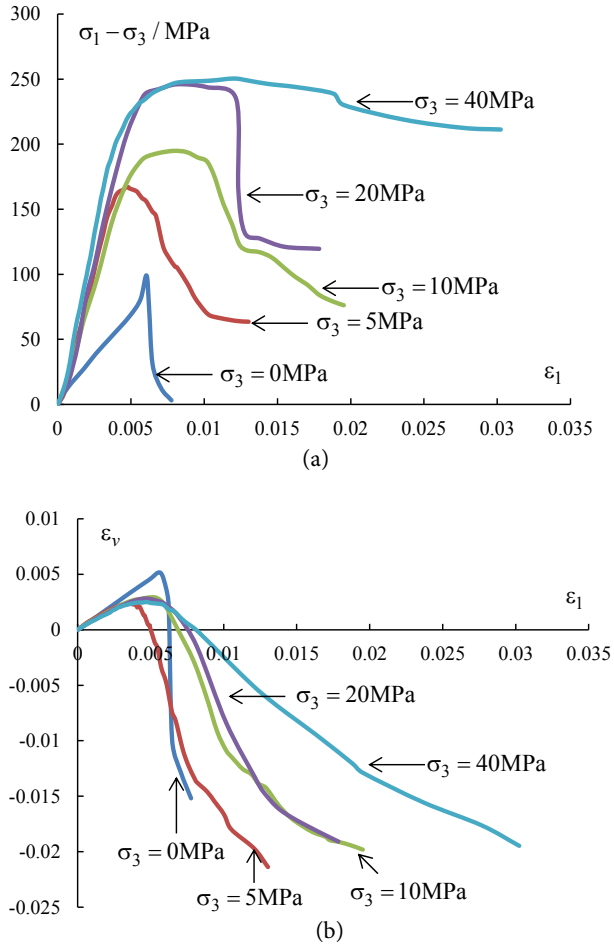


Figure 4. Loading and unloading stress-strain curve under the confining pressure of 5MPa.

curve under the 5MPa confining pressure. The elastic modulus decreases, while the plastic deformation increases with the loading process. As is well known, the weakness of the elastic modulus is related to the evolution of the damage. Thus, the elastoplastic damage evolution is accompanied by the loading process of the T<sub>2b</sub> marble. Fig.5 shows the envelope line for the loading-unloading test curve. The envelope line also stands for the yield surface before the yield and the subsequent yield surface after the yield.



**Figure 5.** Envelope line of the loading-unloading test curve of the T<sub>2b</sub> marble: (a) axial stress–axial strain curve. (b) volumetric strain–axial strain curve.

## 2.2 Test result analysis

The plastic characters in the loading process can be seen from Fig.5: a) The stress-strain test curve is approximately linear under a low confining pressure. The elastic deformation at failure increases with the increasing confining pressure. After a threshold the test curve shows obvious non-linearity and plasticity. b) The confining pressure influences the strength and the

deformation. With the increasing confining pressure, the strength and axial strain increases, while the volumetric strain seems restrained. c) In the case of a low confining pressure, the sample fails in a strain softening character, while strain hardening shows for the high confining pressure. d) There is a transition from volumetric compression to dilation. At first, the micro-fissures were compressed. Then the loading propagates the cracks after a threshold and dilation occurs. However, with the increasing confining pressure, the dilation is slow to happen and appears to be suppressed.

In the meantime, the fissures in the T<sub>2b</sub> marble have such a sequence of evolution due to damage: a) Under low applied loading stress, the microcracks are compressed and the volume decreases. b) With the increasing loading stress, local instability leads to mesoscopic fracture. c) Mesoscopic fracture propagates and extends. d) The mesoscopic fracture develops into the penetrating crack and the sample fails.

To sum up, there is a coupling elastoplastic and damage effect in the loading process of the T<sub>2b</sub> marble. When the load is not large enough, the microfissures are compressed and the material is elastic. With the increasing loading pressure, cracks propagate and dislocation occurs. Plastic deformation induces damage and, conversely, there is a further development of the plastic deformation. Therefore, it is necessary to use the coupled elastoplastic damage theory in the loading analysis of the T<sub>2b</sub> marble[10].

## 3 ELASTOPLASTIC DAMAGE-COUPLING MODEL

There is no obvious anisotropic character in T<sub>2b</sub> marble. So the isotropic theory is used in the analysis. It is presumed that the weakness due to the mesoscopic fissures can be described by the macroscopical isotropic damage. The damage process is defined by the damage variable in a scalar form. Under isothermal conditions, the state variables in the loading process are listed as the total strain tensor  $\epsilon$ , the damage variable  $\omega$ , the elastic strain tensor  $\epsilon^e$  and the plastic strain tensor  $\epsilon^p$ . The full variable form and incremental form of strain can be expressed

$$\epsilon = \epsilon^e + \epsilon^p, d\epsilon = d\epsilon^e + d\epsilon^p \quad (1)$$

It is assumed that there is a thermodynamic potential coupling the damage and plasticity. The thermodynamic potential can be expressed as

$$\psi = \frac{1}{2} \epsilon^e : \mathbb{C}(\omega) : \epsilon^e + \psi_p(\kappa, \omega) \quad (2)$$

where  $\psi_p$  is the thermodynamic potential describing the strain hardening of the damaged material.  $\kappa$  is the internal variable for plastic hardening, which can be described by the plastic deformation, such as the plastic strain or the equivalent plastic shear strain.  $\mathbb{C}(\omega)$  is the fourth order of the elastic tensor. For isotropic material,  $\mathbb{C}(\omega)$  is expressed as [11]

$$\mathbb{C}(\omega) = 2G(\omega)\mathbb{K} + 3K(\omega)\mathbb{J} \quad (3)$$

where  $G$  and  $K$  are the shear modulus and bulk modulus, respectively.  $\mathbb{K}$  and  $\mathbb{J}$  are the isotropic fourth tensor, which can be expressed as

$$\mathbb{K} = \mathbb{I} - \mathbb{J}, \mathbb{J} = \frac{1}{3} \delta \otimes \delta \quad (4)$$

where  $\delta$  is a second-order unit tensor.  $\mathbb{I}$  is a symmetric fourth-order unit tensor. For a second-order tensor  $E$ , we have  $\mathbb{J} : E = \frac{1}{3}(trE)\delta$ ,  $\mathbb{K} : E = E - \frac{1}{3}(trE)\delta$ .

The partial derivative operation is done with equation (2) and we have

$$\sigma = \frac{\partial \Psi}{\partial \varepsilon^e} = \mathbb{C}(\omega) : \varepsilon^e \quad (5)$$

Considering the damage to the elastic parameters, thus equation (5) can be rewritten in incremental form as

$$d\sigma = \mathbb{C}(\omega) : d\varepsilon^e + \frac{\partial \mathbb{C}(\omega)}{\partial \omega} : \varepsilon^e d\omega \quad (6)$$

### 3.1 Damage description

In the framework of the irreversible energy, many damage models have been established. In these models, the damage evolution is determined by the evolution function with a damage variable. The test shows that there is a shear bond penetrating the sample and particles slide along the microcrack with damage evolution. Thus, in this paper the damage driving force  $Y_\omega$  is

$$Y_\omega = \int \sqrt{\frac{2}{3} de : de} \quad (7)$$

where  $de$  is the incremental form of deviatoric strain expressed as  $de = d\varepsilon - \frac{1}{3}(trd\varepsilon)\delta$ .

Inspired by the damage model proposed by Mazars[12], in this paper the damage evolution function is

$$f_\omega = \omega - \omega_{\max} \left( 1 - \frac{1}{\exp[B_c(Y_\omega - Y_{\omega 0})]} \right) = 0 \quad (8)$$

where  $\omega_{\max}$  is the maximum damage variable. The parameter  $B_c$  controls the kinetics of the compressive damage

and can be determined by using a uniaxial compression test. The parameter  $Y_{\omega 0}$  is the damage threshold. To sketch the damage evolution during the loading process, the damage-evolution curve for the T<sub>2b</sub> marble under a confining pressure of 40MPa is shown in Fig.6.

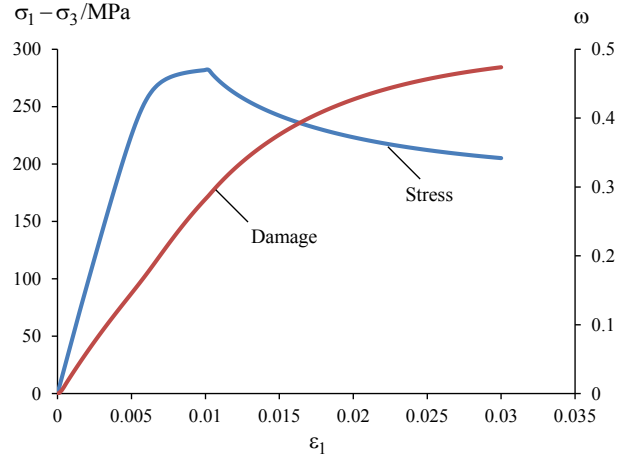


Figure 6. Damage-evolution curve for T<sub>2b</sub> marble under confining pressure of 40MPa.

### 3.2 Plasticity description

According to the test research, rock has the characteristic of pressure sensitivity[13]. In other words, the strength increases with the increasing confining pressure or hydrostatic pressure. In this paper, the value of the variable is positive when the stress is tensile. Inspired by Chen et al., the strength criterion is adopted as

$$c_1 \frac{q}{g(\theta)f_{c0}} + c_2 \left( \frac{q}{g(\theta)f_{c0}} \right)^2 - \left( c_3 - \frac{p}{f_{c0}} \right) = 0 \quad (9)$$

where  $p$  is the hydrostatic pressure expressed as  $p = \frac{1}{3} tr(\sigma)$ .  $q$  is the equivalent shear stress expressed as

$q = \sqrt{\frac{3}{2}} S : S$ .  $S$  is the deviatoric shear tensor expressed as  $S = \sigma - \frac{1}{3}(tr\sigma)\delta$ .  $f_{c0}$  is the uniaxial strength determined by the uniaxial test. The parameters  $c_1$ ,  $c_2$  and  $c_3$  define the curvature of the failure surface and can be determined by plotting the failure surface.  $g(\theta)$  determines the effect of the Lode angle on the strength. In the loading path in this paper,  $g(\theta)$  is simplified as  $g(\theta)=1$ . It is noted that equation (9) is the Drucker-Prager criterion in the case of  $c_2=0$  for the simplified calculation.

The loading equation similar to equation (9) is

$$f_s = q - \alpha_s g(\theta) \bar{\sigma}_c = 0 \quad (10)$$

where  $\bar{\sigma}_c = \frac{(-c_1 + \sqrt{c_1^2 + 4c_2(c_3 - p/f_{c0})})}{2c_2} f_{c0}$ .

$\alpha_s = \alpha_0 + (1 - \alpha_0) \frac{\gamma_p}{B + \gamma_p}$ .  $\alpha_0$  controls the threshold of plasticity.  $B$  controls the kinetics of the compressive plasticity, which is determined by the evolution law of  $\alpha_s$  and  $\gamma_p$ .  $\gamma_p$  is the equivalent plastic shear strain expressed as

$$\gamma_p = \int \sqrt{\frac{2}{3} de^p : de^p} \quad (11)$$

$$de^p = d\varepsilon^p - \frac{1}{3} (tr d\varepsilon^p) \delta \quad (12)$$

when  $\gamma_p \rightarrow 0$ ,  $\alpha_s \rightarrow \alpha_0$ . For  $\gamma_p \rightarrow \infty$ ,  $\alpha_s \rightarrow 1$ .

The generation of microcracks is accompanied by the plastic deformation. To express the weakness the loading function is expressed as

$$f_s = q - \alpha_s g(\theta) \frac{\left(-c_1 + \sqrt{c_1^2 + 4c_2(c_3 - p / \bar{f}_{c0})}\right)}{2c_2} \bar{f}_{c0} = 0 \quad (13)$$

where  $\bar{f}_{c0} = f_{c0} (1 - \langle \omega - \omega_f \rangle)$ ,  $\omega_f$  is the threshold of the damage to the plasticity. When the damage variable is larger than  $\omega_f$ , the loading curve shrinks and the strength decreases. The symbol  $\langle x \rangle$  is expressed as:  $\langle x \rangle = 0$  when  $x \leq 0$  and  $\langle x \rangle = x$  when  $x > 0$ .

The test shows that the volumetric deformation changes from compression to dilation and this effect decreases with the increasing confining pressure. To express the deformation character, inspired by the work [14, 15], the plastic potential function is

$$g_s = q + \mu_s g(\theta) I \ln \left( \frac{I}{I_0} \right) = 0 \quad (14)$$

where  $I = -p + c_3 \bar{f}_{c0}$ . The parameter  $I_0$  determines the intersection point of the plastic potential surface and the coordinate  $p$ . The threshold of the volumetric compression to dilation can be determined by  $\frac{\partial g_s}{\partial I} = 0$ , expressed as

$$f_{sw} = q - \mu_s g(\theta) (-p + c_3 \bar{f}_{c0}) = 0 \quad (15)$$

where the parameter  $\mu_s$  defines the slope of the boundary between the compressibility and dilatancy domains. Its value can be obtained by plotting the transition boundary line in the  $p$ - $q$  plane.

### 3.3 The damage and plasticity coupling numerical process

In a general loading path, the plastic flow and damage evolution can be activated regarding the loading law, respectively. There are two kinds: a)  $d\omega > 0, f_s = 0$ . b)  $d\omega > 0, f_s < 0$ .

#### 3.3.1 (a) $d\omega > 0, f_s = 0$

In this case, the plastic flow and the damage evolution are activated. The damage variable increment is determined by

$$\begin{aligned} d\omega &= d\lambda_\omega \frac{\partial f_\omega}{\partial Y_\omega} \\ &= d\lambda_\omega \frac{-\omega_{\max} B_c}{\exp[B_c(Y_\omega - Y_{\omega 0})]} \end{aligned} \quad (16)$$

where  $d\lambda_\omega$  is the damage multiplier, which can be determined by the damage-consistency condition

$$\begin{aligned} df_\omega &= \frac{\partial f_\omega}{\partial Y_\omega} dY_\omega + \frac{\partial f_\omega}{\partial \omega} d\omega \\ &= \frac{-\omega_{\max} B_c}{\exp[B_c(Y_\omega - Y_{\omega 0})]} \left( \frac{\partial Y_\omega}{\partial \varepsilon^e} : d\varepsilon^e + \frac{\partial Y_\omega}{\partial \varepsilon^p} : d\varepsilon^p \right) + d\omega = 0 \end{aligned} \quad (17)$$

From equations (16) and (17) we have

$$d\lambda_\omega = - \left( \frac{\partial Y_\omega}{\partial \varepsilon^e} : d\varepsilon^e + \frac{\partial Y_\omega}{\partial \varepsilon^p} : d\varepsilon^p \right) \quad (18)$$

For plasticity, the plastic strain increment is

$$d\varepsilon^p = d\lambda_s \frac{\partial g_s}{\partial \sigma} \quad (19)$$

where  $d\lambda_s$  is the plastic multiplier, which can be determined by the plastic consistency condition as

$$df_s = \frac{\partial f_s}{\partial \sigma} : d\sigma + \frac{\partial f_s}{\partial \gamma_p} \frac{\partial \gamma_p}{\partial \varepsilon^p} : d\varepsilon^p + \frac{\partial f_s}{\partial \omega} d\omega = 0 \quad (20)$$

From equations (19) and (20), the plastic multiplier is determined as

$$d\lambda_s = - \frac{\frac{\partial f_s}{\partial \sigma} : d\sigma + \frac{\partial f_s}{\partial \omega} d\omega}{\frac{\partial f_s}{\partial \gamma_p} \frac{\partial \gamma_p}{\partial \varepsilon^p} : \frac{\partial g_s}{\partial \sigma}} \quad (21)$$

Substitute (16) into (21) and (19) into (18), the simultaneous equations are obtained and thus we get the plastic multiplier and the damage multiplier. The constitutive function in incremental form can be expressed as

$$\begin{aligned} d\sigma &= \mathbf{C}(\omega) : \left( d\varepsilon - d\lambda_s \frac{\partial g_s}{\partial \sigma} \right) \\ &- d\lambda_\omega \frac{\omega_{\max} B_c}{\exp[B_c(Y_\omega - Y_{\omega 0})]} \frac{\partial \mathbf{C}(\omega)}{\partial \omega} : \varepsilon^e \end{aligned} \quad (22)$$

#### 3.3.1 (b) $d\omega > 0, f_s < 0$

For  $f_s < 0$ , the stress point is in the elastic range and no plastic flow happens.  $d\omega > 0$  and there is only damage evolution. Accordingly, the plastic strain increment is

0. Therefore,  $d\varepsilon^p=0$ . The damage-variable increment is expressed as equation (16). Similar to equation (17), the damage-consistency condition is expressed as

$$df_{\omega} = \frac{\partial f_{\omega}}{\partial Y_{\omega}} dY_{\omega} + \frac{\partial f_{\omega}}{\partial \omega} d\omega \quad (23)$$

$$= \frac{-\omega_{\max} B_c}{\exp[B_c(Y_{\omega} - Y_{\omega 0})]} \left( \frac{\partial Y_{\omega}}{\partial \varepsilon^e} : d\varepsilon^e \right) + d\omega = 0$$

From equation (16) and (23), the damage multiplier is derived

$$d\lambda_{\omega} = -\frac{\partial Y_{\omega}}{\partial \varepsilon^e} : d\varepsilon^e \quad (24)$$

For the elastic strain to equal the total strain in the elastic loading, that is

$$d\varepsilon^e = d\varepsilon \quad (25)$$

From equations (24) and (25) we get

$$d\lambda_{\omega} = -\frac{\partial Y_{\omega}}{\partial \varepsilon} : d\varepsilon \quad (26)$$

Thus, the constitutive equation is

$$d\sigma = \mathbb{C}(\omega) : d\varepsilon - d\lambda_{\omega} \frac{\omega_{\max} B_c}{\exp[B_c(Y_{\omega} - Y_{\omega 0})]} \frac{\partial \mathbb{C}(\omega)}{\partial \omega} : \varepsilon \quad (27)$$

## 4 NUMERICAL SIMULATION AND VALIDATION

The parameters in the model are determined in three steps. a) The plastic parameters are determined by only considering the plastic mechanism. b) The damage parameters are determined with the plastic parameters. c) The plastic parameters are adjusted according to the failure. In the model, the last step accomplishes coupling the damage and plastic by introducing  $\bar{f}_{c0}$  in equation (13). In details, the parameters of the model can be determined by the test following the steps: a) The uniaxial compressive strength  $f_{c0}$  is determined by the uniaxial compression test. b) Neglecting damage process, at the initial yield, no plasticity formulates. For simplicity, the peak strength in the triaxial compression test with different confining pressures is viewed as an initial yield stress. The yield criterion parameters  $c_1$ ,  $c_2$  and  $c_3$  could be determined by using equation (9) according to the peak strength. c) After the initial yield, plasticity formulates with the plastic deformation represented by  $\gamma_p$ . According to the strain-hardening phase, the parameter  $B$  can be obtained by the evolution law of  $\alpha_s(\gamma_p)$ . d) Find out the stress with the corresponding volumetric strain rate equal to zero. The stress state means a transition from the volumetric compressibility

to the dilatancy. The transition boundary line between the compressibility and dilatancy domains is sketched in the  $p$ - $q$  plane and the parameter  $\mu_s$  is obtained. e) The damage parameters are considered after the determination of the plastic parameters. The softening phase is dominated by the damage in equation (13). With the softening stress-strain test data, the damage-evolution law and the parameter  $B_c$  are determined.

The triaxial test of the T<sub>2b</sub> marble is simulated using the proposed model. The parameters in the model are listed in Table 1. Fig.7 shows the consistency between the simulation result and test curve. According to the simulation results it can be inferred: a) Brittleness is more obvious under a low-confining pressure. The stress falls down after the peak in the strength. In this condition the damage mechanism generally works (see Fig.7(a)). b) The ductile character is revealed under a high confining pressure. There is no obvious stress fall after the peak strength. In this case the plastic mechanism generally works (see Fig.7(c)). c) The strength and strain increase with the increasing confining pressure. d) There is a transition between the volumetric compression and the dilation. The dilation under the confining pressure 40MPa is not as obvious as 5MPa. The confining pressure restrains the dilation. Fig.8 shows the loading and unloading test and simulation results. The hysteresis loop occurred in the compression phase of the cyclic loading and unloading test. This loop results from the frictional movement of the particles during the cyclic loading and unloading. Because in the proposed model there is no plasticity and damage accumulation, the re-loading curve coincides with the unloading diagram. Both the simulation and test represent the elastic stiffness decrease in the loading process. There is a deviation between the simulation result and test curve, but the proposed model can express the mechanical characters of the brittle hard rock in a qualitative manner. This would have significance for a stability analysis of deep buried tunnels.

**Table 1.** Parameters in the proposed model.

Parameter type	Parameter value
Elastoplastic parameter	$f_{c0} = 99\text{MPa}$
	$c_1 = 0.2$
	$c_2 = 0.1$
	$c_3 = 0.05$
	$B = 9 \times 10^{-5}$
Damage parameter	$\mu_s = 1.4$
	$B_c = 85$

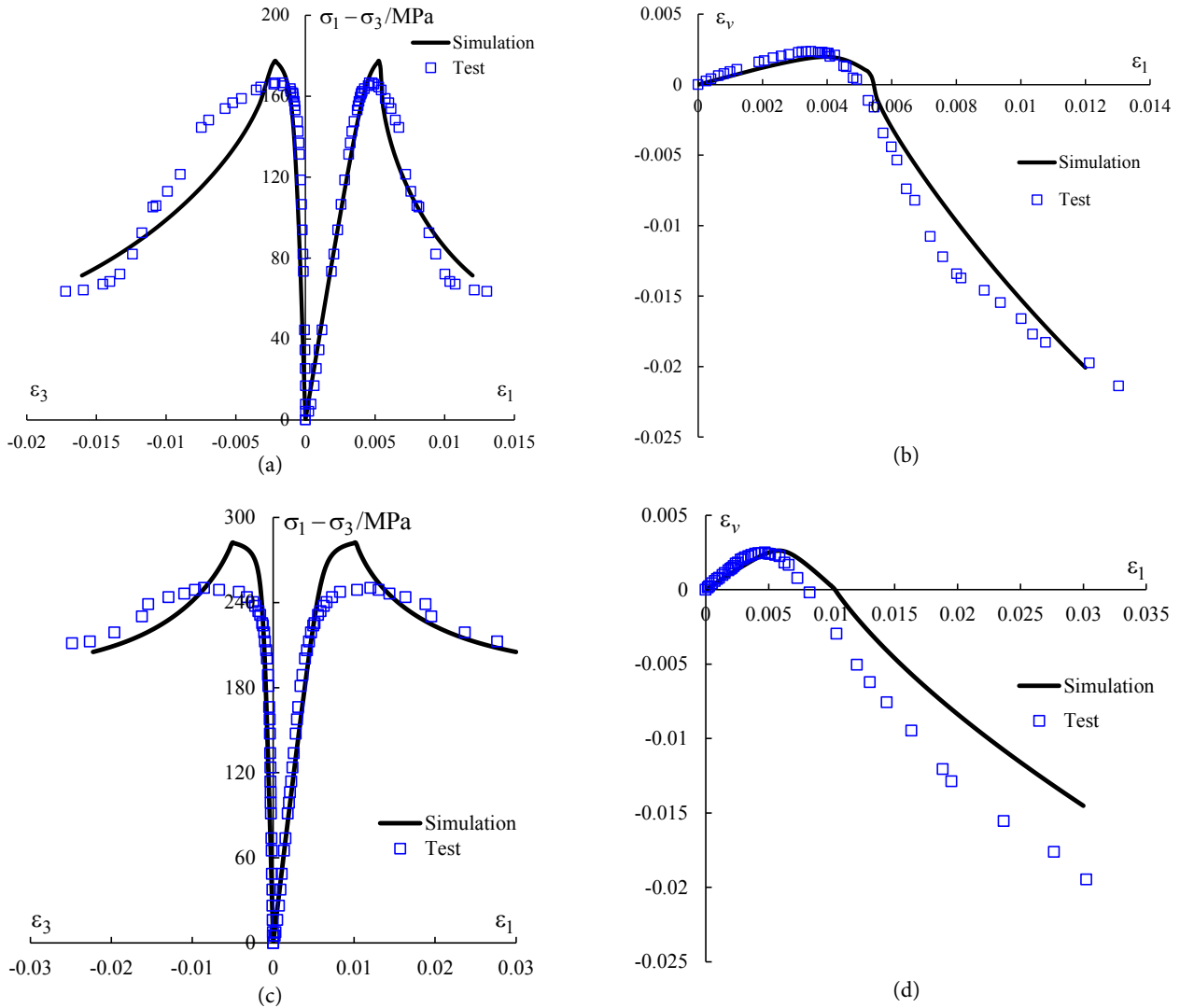


**Figure 7.** Simulation results and test curves: (a) axial stress-axial strain curve under confining pressure of 5MPa. (b) volumetric strain-axial strain curve under confining pressure of 5MPa. (c) axial stress-axial strain curve under confining pressure of 40MPa. (d) volumetric strain-axial strain curve under confining pressure of 40MPa.

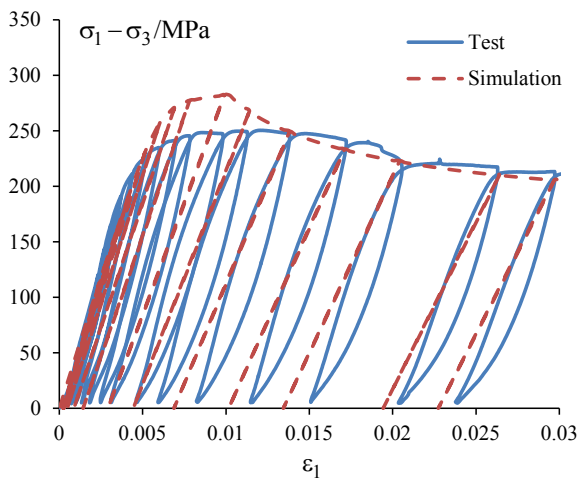


**Figure 8.** Simulation and test results of the loading and unloading process.

## 5 CONCLUSIONS

A tri-axial test is conducted in an analysis of deep buried  $T_{2b}$  marble. The hard rock in this study shows obvious pressure sensitivity and dilation. The strength and failure strain increase with the increasing confining pressure. At the same time, the dilation is suppressed and the non-linear character becomes more obvious. Based on the influence of the damage and plastic mechanism in the test, the damage-evolution function is proposed to reflect the mechanical weakness with the damage. Considering the influence of damage on the plasticity, the plastic-loading function and the plastic potential function are established. According to the activation law of the damage and plasticity, the elastoplastic damage constitutive function is proposed. The parameters of the

model are determined using a conventional tri-axial test. Then the model is verified by a simulation of the test curve. The proposed model can express the mechanical characters of deep buried hard rock in an accurate way.

## Acknowledgments

We gratefully acknowledge financial support from National Natural Science Foundation of China (NSFC) (51704097), the Project of Key Opening Laboratory for Deep Mining Construction at Henan province (2015 KF-06), the Key Scientific Research Project of Henan Higher Education Institutions (16A560004), Dr. Fund Projects of Henan Polytechnic University (B2016-65) and the cooperative program between HPU and UL.

## REFERENCES

- [1] Zhou, H., Zhang, C.Q., Li, Z., et al. 2014. Analysis of mechanical behavior of soft rocks and stability control in deep tunnels. *Journal of Rock Mechanics and Geotechnical Engineering* 6(3), 219-226. DOI: 10.1016/j.jrmge.2014.03.003
- [2] Zhang, C.S., Liu, N., Chu, W.J. 2016. Key technologies and risk management of deep tunnel construction at Jinping II hydropower station. *Journal of Rock Mechanics and Geotechnical Engineering* 8(4), 499-512. DOI: 10.1016/j.jrmge.2015.10.010
- [3] Li, Z., Zhou, H., Song, Y.Z., et al. 2013. Mechanical model of chlorite schist considering hardening-softening and dilatancy characteristics. *Rock and Soil Mechanics* 34(2), 404-410. DOI: 10.16285/j.rsm.2013.02.017
- [4] Singh, M., Raj, A., Singh, B. 2011. Modified Mohr-Coulomb criterion for non-linear triaxial and polyaxial strength of intact rocks. *International Journal of Rock Mechanics and Mining Sciences* 48(4), 546-555. DOI: 10.1016/j.ijrmms.2011.02.004
- [5] Cicekli, U., Voyiadjis, G.Z., Al-Rub, R.K.A. 2007. A plasticity and anisotropic damage model for plain concrete. *International Journal of Plasticity* 23(10), 1874-1900. DOI: 10.1016/j.ijplas.2007.03.006
- [6] Salari, M.R., Saeb, S., Willam, K.J., et al. 2004. A coupled elastoplastic damage model for geomaterials. *Computer Methods in Applied Mechanics and Engineering* 193(27), 2625-2643. DOI: 10.1016/j.cma.2003.11.013
- [7] Chiarelli, A.S., Shao, J.F., Hoteit, N. 2003. Modeling of elastoplastic damage behavior of a claystone. *International Journal of Plasticity* 19(1), 23-45. DOI: 10.1016/S0749-6419(01)00017-1
- [8] Zhu, Q.Z., Shao, J.F., Mainguy, M. 2010. A micromechanics-based elastoplastic damage model for granular materials at low confining pressure. *International Journal of Plasticity* 26(4), 586-602. DOI: 10.1016/j.ijplas.2009.09.006
- [9] Zhou, C.Y., Zhu, F.X. 2010. An elasto-plastic damage constitutive model with double yield surfaces for saturated soft rock. *International Journal of Rock Mechanics and Mining Sciences* 47(3), 385-395. DOI: 10.1016/j.ijrmms.2010.01.002
- [10] Zhou, H., Zhang, K., Feng, X.T. 2011. A coupled elasto-plastic-damage mechanical model for marble. *Science China Technological Sciences* 54(1), 228-234. DOI: 10.1007/s11431-011-4642-3
- [11] Chen, W.F., Saleeb, A.F. 1994. *Constitutive equations for engineering materials: elasticity and modeling*. Elsevier, Amsterdam.
- [12] Mazars, J. 1984. *Application de la mécanique de l'endommagement au comportement non linéaire et à la rupture du béton de structure*. Université Paris VI, France.
- [13] Aubertin, M., Li, L., Simon, R., et al. 1999. Formulation and application of a short-term strength criterion for isotropic rocks. *Canadian Geotechnical Journal* 36(5), 947-960. DOI: 10.1139/t99-056
- [14] Shao, J.F., Jia, Y., Kondo, D., et al. 2006. A coupled elastoplastic damage model for semi-brittle materials and extension to unsaturated conditions. *Mechanics of Materials* 38(3), 218-232. DOI: 10.1016/j.mechmat.2005.07.002
- [15] Jia, Y., Bian, H.B., Su, K., et al. 2010. Elastoplastic damage modeling of desaturation and resaturation in argillites. *International Journal for Numerical and Analytical Methods in Geomechanics* 34(2), 187-220. DOI: 10.1002/nag.819